**Global Spatial Deconvolution of Lunar Prospector Th Abundances Using the Pixon and Jansson Deconvolution Methods.** D. J. Lawrence[1], R. C. Puetter[2,3], R. C. Elphic[1], W. C. Feldman[1], J. J. Hagerty[1], T. H. Prettyman[1], and P. D. Spudis[4], [1]Los Alamos National Laboratory, Los Alamos, NM (djlawrence@lanl.gov). [2]University of California, San Diego, CA. [3]PixonImaging LLC, San Diego, CA. [4]Johns Hopkins Applied Physics Laboratory, Laurel, MD.

**Introduction:** The global distribution of lunar Th abundances measured by the Lunar Prospector Gamma-ray Spectrometer (LP-GRS) [1,2] has significantly enhanced our understanding of the Moon's formation and evolution [3]. For example, Jolliff et al., [4] used global Th data to suggest that instead of the mare/highlands dichotomy, the Moon should be thought of as three geochemical provinces comprised of a nearside high-Th terrane, a low-Th feldspathic highlands terrane, and the South Pole-Aitken basin floor. While the LP-GRS data have shed new light on large scale lunar geochemistry, the characteristically broad spatial resolution of the LP-GRS data (80 km) makes it difficult to determine the Th abundances of small-scale geologic features. To address this issue, forward modeling techniques have been used to improve our understanding of the Th abundances of small features [2,5,6]. However, these methods rely on other sources of data and it is desirable to achieve improved spatial resolution entirely internal to the LP dataset.

Spatial deconvolution offers a way to improve the spatial resolution of the LP dataset if the spatial response function and statistical uncertainties of the data are sufficiently well known. Here, we describe the results of a study [7] where we compare two different deconvolution techniques – Jansson's method and the Pixon method – using LP-GRS Th data. We conclude that the Pixon method produces significantly improved deconvolved maps, which we use to revisit geologically complex regions, such as the Aristarchus Plateau.

**Spatial Deconvolution Techniques:** Spatial deconvolution is a well developed field with some of the early work being carried out in the early 1900s [8]. For our purpose, we define the objective of spatial deconvolution as enhancing the spatial contrast and resolution of the image data to the limit allowed by the noise characteristics of the data. Spatial deconvolution techniques have been applied to a variety of data sets ranging from laboratory microscopy, visible imaging, and telescopic astrophysical observations. Improvements in spatial resolution of factors of two to three have been achieved in some applications [9]. However, despite the potential improvement provided by spatial deconvolution, all spatial deconvolution techniques must trade off the improvement in spatial resolution with the amplification of noise present in all data. Different techniques use various methods to trade off the competing goals of improving spatial resolution but reducing noise-induced artifacts.

Jansson's method is a non-linear, iterative technique that has been described elsewhere [7,10]. It has the advantage that it is relatively easy to implement and produces reasonable results [10]. The Pixon method is a spatially adaptive, image restriction method that is one of a class of deconvolution techniques that seeks the smoothest possible image as constrained by both the original data and the data uncertainty [9]. A unique feature of the Pixon method is that it uses variably sized smooth patches, or Pixon elements, within the image in order to express the information content of the image. For example, if the variation within a large portion of the image can be attributed solely to noise, then the size of the Pixon element in this region would be relatively large. In contrast, regions containing statistically significant small-scale spatial variations will have smaller Pixon element sizes that capture larger amounts of information. In general, a set of Pixon elements for a given image represents the minimum set required to describe the image information content within the limits allowed by the noise [9].

**Results:** Fig. 1 shows the results of the two deconvolution algorithms for a nearside region including Copernicus and Fra Mauro. Fig. 1a shows the original Th data, Fig. 1b shows the Jansson deconvolved map, and Fig. 1c shows the Pixon deconvolved map. For both of the deconvolved maps, there is a clear sharpening of the image compared to the original map. In addition, the deconvolved maps resolve some small-scale features identified in other studies such as the Lassell and Gruithuisen red spots [6]. However, we note that the Jansson deconvolved map shows high-frequency spatial variations that are indicative of noise artifacts. Such high-frequency variations are not as strongly seen in the Pixon deconvolved map. There are also clear indications from the residuals (not shown) that the Jansson method results in an image with significantly more biases and artifacts than the Pixon method (the residuals $R$ are defined as $R = (D - P \otimes I)/s$, where $D$ is the original data, $P$ is the point spread function, $I$ is the deconvolved image, and $s$ is the image uncertainties). We therefore conclude that the Pixon method gives much better results than the Jansson method.

Fig. 2 shows a global nearside map where the Th abundances have been deconvolved using the Pixon method. This map was constructed using ~900 x 900 km sized regions (i.e., 60° x 60° equivalent size at the equator) that were combined together to create the map shown. The absolute Th abundances were derived by correlating the deconvolved counting rate with the Th abundances of Prettyman et al., [11] in a manner similar to what was done for the smoothed Th map of Lawrence et al., [2].

There are a number of features in the deconvolved map whose spatial contrast is significantly enhanced compared to the original data [2]. For example, the craters Plato and Copernicus are clearly delineated from their surrounding regions as Th lows and these data show that the Th abundances within these craters are ~2 – 3 ppm compared to the >4 – 5 ppm values seen in the original map. There are also a number of locations in the Fra Mauro region that show strong correlation with spectrally derived, high spatial resolution FeO data [12], which provide confidence in the validity of the deconvolved data [10].

Finally, Fig. 3 shows a regional view of the Aristarchus region. These data show a Th enhancement at Aristarchus crater with lower abundances to the NW over the Aristarchus plateau. In the deconvolved map (Fig. 3b), the Th abundances in the plateau show a lane of low values co-located with a region of relatively high iron abundances (14-18 wt.% FeO [12]) that appear to be associated with the Agricola Straits. There is also a new, separate enhancement of high Th associated with the Agricola Mountains. Neither the low-Th lane nor the NW enhancement were seen in the original low resolution Th data (Fig. 3a). The new map shows that this NW Th enhancement is not related to Th-rich impact ejecta from Aristarchus Crater and suggests that high-Th lithologies make up at least part of the Agricola Mountains.

**References:** [1] Lawrence et al., *Science*, 284, 1484, 1998. [2] Lawrence et al., *JGR*, 10.1029/2001JE001530, 2003. [3] Jolliff et al., New Views of the Moon, *Rev. in Min. and Geochem.*, Vol. 60, 2006. [4] Jolliff et al., *JGR.*, 105 (#E2), 4197, 2000. [5] Lawrence et al., *GRL*, 10.1029/2004 GL022022, 2005. [6] Hagerty et al., *JGR.*, 111, 10.1029/2005JE002592, 2006. [7] Lawrence et al., *GRL*, 10.1029/2006GL028530, in press, 2007. [8] Van Cittert, *Z. Phys.*, 69, 298, 1931. [9] Puetter et al., *Ann. Rev. Astron. Astrophys.*, 43, 139, 2005. [10] Lawrence et al., 37th *LPSC, #1915*, 2006. [11] Prettyman et al., *JGR*, 111, 10.1029/2005JE002656, 2006. [12] Lucey et al., *JGR.*, 105, #E8, 20297, 2000.

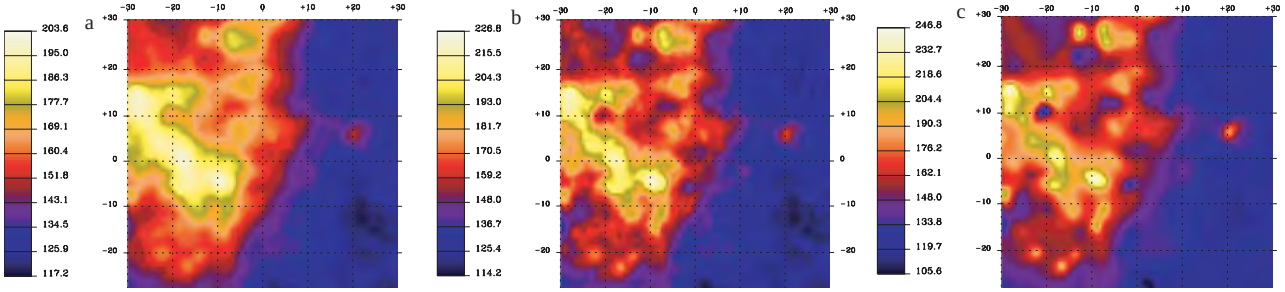


**Figure 1.** a) Original Th map from Lawrence et al., [2003] for 30°W - 30°E and 30°S - 30°N; b) Deconvolved map using Jansson's method; c) Deconvolved map using the Pixon method. All maps are given in units of counts per 32 seconds.

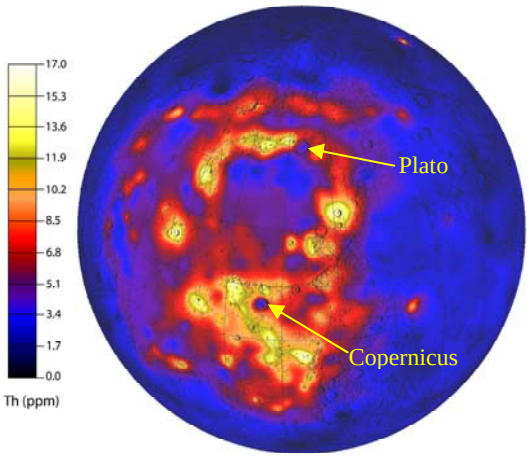


**Figure 2.** Nearside map of Pixon deconvolved Th abundances.

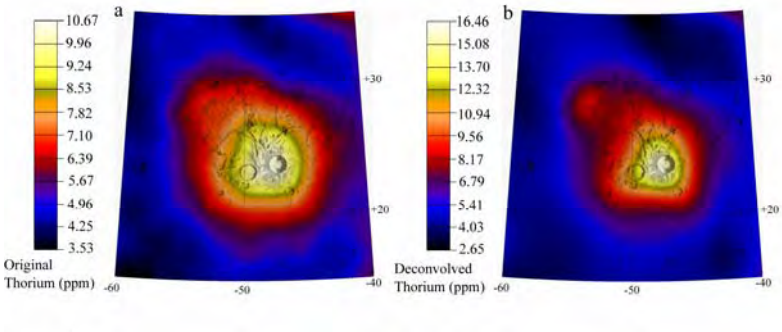


**Figure 3.** a) Original Th abundances at Aristarchus crater; b) Pixon deconvolved Th abundances at Aristarchus crater.